Electronic Supplementary Material (ESI) for Catalysis Science & Technology.
This journal is © The Royal Society of Chemistry 2017

Supporting information

Cu Supported on Thin Carbon Layer Coated Porous SiO_2 for Efficient Ethanol Dehydrogenation

Qing-Nan Wang,[a] Lei Shi,[a] Wei Li,[b] Wen-Cui Li,[a] Rui Si,[b] Ferdi Schüth,[c] and An-Hui Lu*[a]

[a] State Key Laboratory of Fine Chemicals, School of Chemical Engineering, Dalian University of Technology, Dalian 116024, P. R. China. E-mail: anhuilu@dlut.edu.cn

[b] Shanghai Synchrotron Radiation Facility, Shanghai Institute of Applied Physics, Chinese Academy of Sciences, Shanghai, 201204, China

[c] Max-Planck-Institut für Kohlenforschung, Kaiser-Wilhelm-Platz 1, D-45470 Mülheim an der Ruhr, Germany

E-mail: anhuilu@dlut.edu.cn

Contents

1. TEM images of C/SiO_2 and $Cu/C/SiO_2$ Page S3
2. TEM images of Cu/SiO_2 and Cu/C Page S4
3. XRD patterns of the catalysts Page S5
4. N_2 adsorption–desorption isotherms Page S6
5. XRD patterns of the supports Page S7
6. The calculation of carbon consumption Page S8
7. Raman spectra Page S9
8. XPS data Page S10
9. CO-DRIFTS spectra Page S11
10. Stability test Page S12
11. Dependence of product selectivity and ethanol conversion on W/F Page S13
12. CH_3CHO-TPD profiles Page S14
13. Summary of the catalytic data of Cu-based catalysts Page S15
14. References Page S17

1 TEM images of C/SiO_2 and $Cu/C/SiO_2$

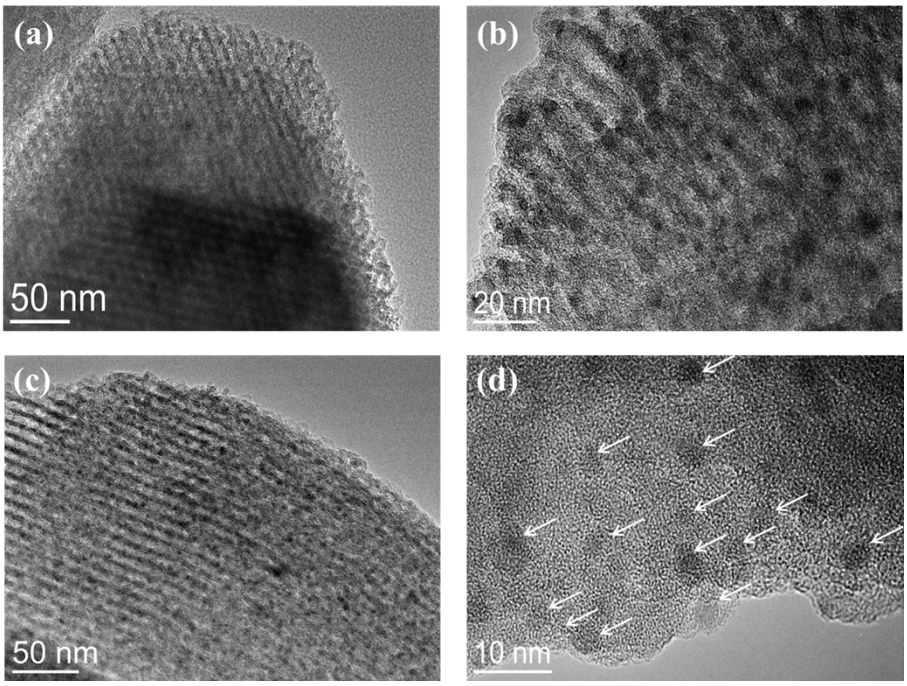

Fig. S1 (a) and (b) TEM images of C/SiO_2 support, (c) and (d) TEM images recorded at different magnifications of the reduced $Cu/C/SiO_2$ catalysts. In panel d, the Cu particles were highlighted by white arrows.

It is difficult to distinguish the carbon layer from the SiO_2 matrix in the above images due to their similar atomic number (near Z-contrast) and the thin thickness of carbon layer (~0.5 nm).

2 TEM images of Cu/SiO_2 and Cu/C

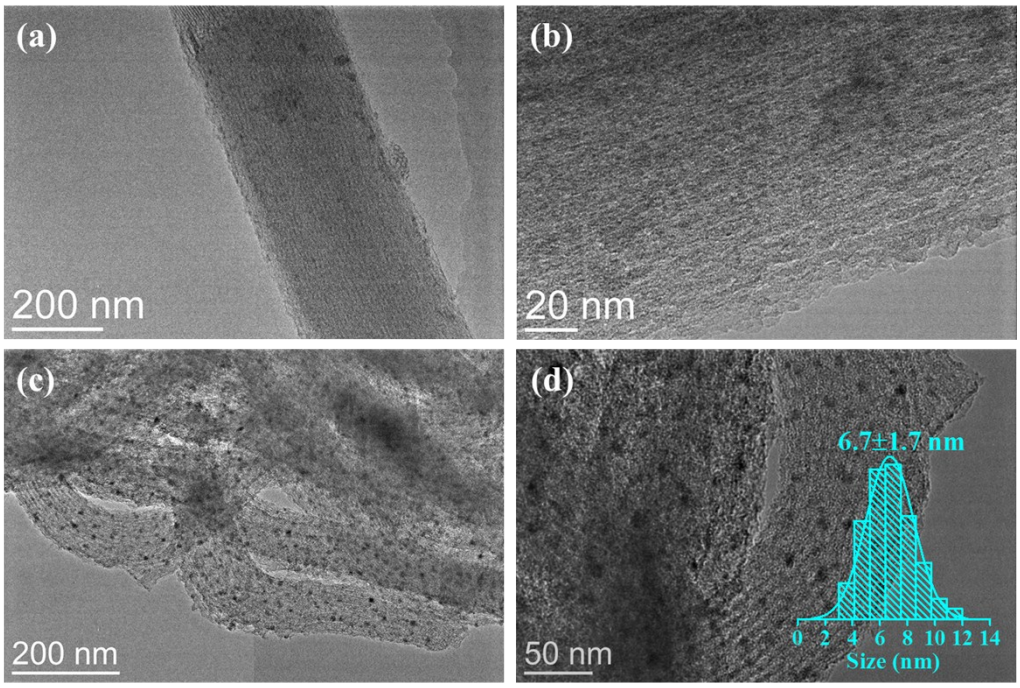

Fig. S2 TEM images for the reduced Cu/SiO_2 (a and b) and Cu/C (c and d).

3 XRD patterns of the catalysts

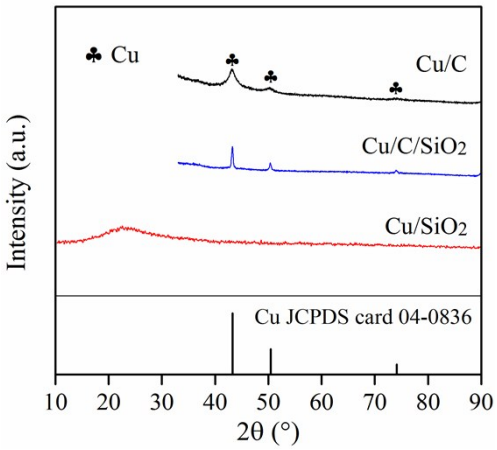

Fig. S3 XRD diffraction patterns of the catalysts.

From the HS-LEIS results, ca. 7% Cu particles located at the outside of the pores on Cu/C/SiO_2. In the high reduction temperature, these Cu species may more easily agglomerate, and show a larger metal size than those in the mesopores. So the mean size of Cu NPs may be overestimated by using a Scherrer equation based on the XRD patterns. This phenomenon was also reported by K. P. de Jong et.al,[1] who suggested that there is a small amount of relatively large Cu nanoparticles on the Cu-based catalysts. In this case, the mean diameter of Cu particles was calculated by using N_2O-H_2 titration method based on the consumption amount of H_2, which will provide more reliable particle size information.

In the case of Cu/SiO_2, although there are 15% Cu species outside the pores, they easily interact with the SiO_2 surface due to the direct contact. Hence, the distribution of Cu particles on SiO_2 is uniform. As Cu nanoparticles on oxide tend to be oxidized to a higher valence and monolayer dispersion[2] as soon as exposing to the air atmosphere (including O_2 and moisture) during analysis. So to Cu/SiO_2 catalyst, N_2O-H_2 titration method to analyze Cu particle size is also well-adopted.

4 N_2 adsorption–desorption isotherms of the supports

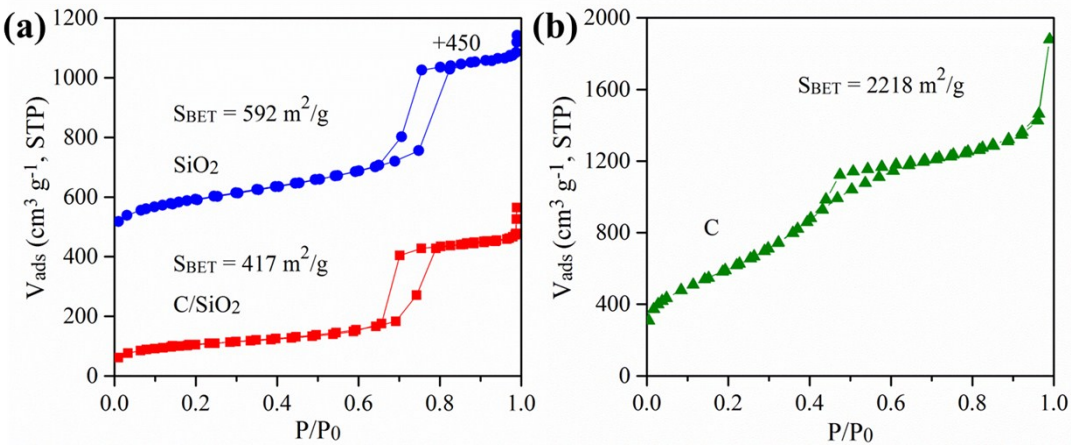

Fig. S4 N_2 adsorption–desorption isotherms of SiO_2, C/SiO_2, and C supports. The isotherm of SiO_2 is vertically offset by +450 cm^3 g^{-1}, STP.

5 XRD patterns of the supports

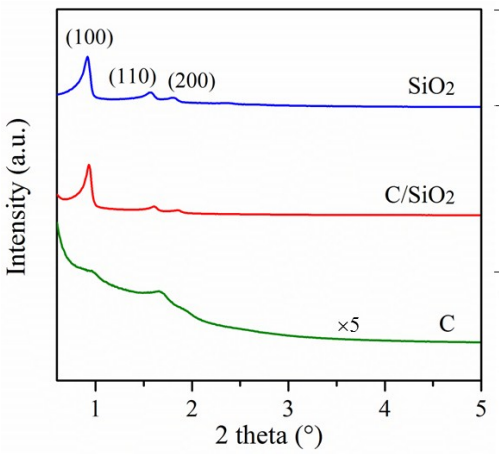

Samples	d (100) or d(110) /nm	Wall Thickness /nm
SiO_2	9.526	3.4
C/SiO_2	9.526	4.5
C	9.370	1.2

Wall thickness: $2\times d_{100}/3^{1/2}$-pore size for SiO_2 and C/SiO_2; $2\times d_{110}/3^{1/2}$-pore size for C.

Fig. S5 Low angle XRD patterns of the supports and corresponding calculated results.

6 The calculation of carbon consumption

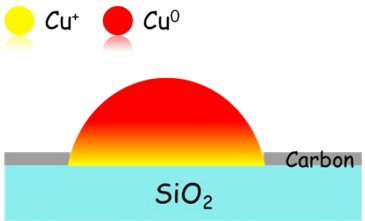

Fig. S6 The model of Cu/C/SiO_2 catalysts after a methanation process of the carbon layer under a hydrogen atmosphere.

We assumed that the Cu NPs are rigid hemisphere, *i.e.*, the morphology and diameter remain unchanged before and after the methanation of carbon. The carbon consumption m_C etched by Cu nanoparticles was calculated as the following:

1) The density ρ of carbon layer:

$$\rho = Q \div (S_{BET} \times h) = \frac{86 \div 1000 g / g}{417 m^2 / g \times (7.6 - 6.5) \times 10^{-9} \div 2m} = \sim 0.37\ g/cm^3$$

Q: the carbon content of C/SiO_2; S_{BET}: the surface area of C/SiO_2; h: the thickness of carbon layer.

2) The number of Cu nanoparticles per 100 mg catalyst:

$$N = m_{Cu} \div (V_{Cu} \times \rho_{Cu}) = \frac{8.8 \div 1000 g}{0.5 \times \frac{4}{3}\pi (1.1 \times 10^{-9} m)^3 \times 8.96 \times 10^6 g / m^3} = \sim 0.35 \times 10^{18}$$

m_{Cu}: the Cu loading on C/SiO_2; V_{Cu}: the volume of a single Cu particle, the diameter is based on the dispersion data; ρ_{Cu}: the density of Cu metal, 8.96 g/cm^3.

3) The carbon consumption m_C per 100 mg catalyst:

$$m_C = \pi R^2 \times N \times h \times \rho =$$

$$\pi \times (1.1 \times 10^{-9} m)^2 \times 0.35 \times 10^{18} \times 0.5 \times 10^{-9} m \times 0.37 \times 10^6 g / m^3 = \sim 0.24\ mg$$

7 Raman spectra

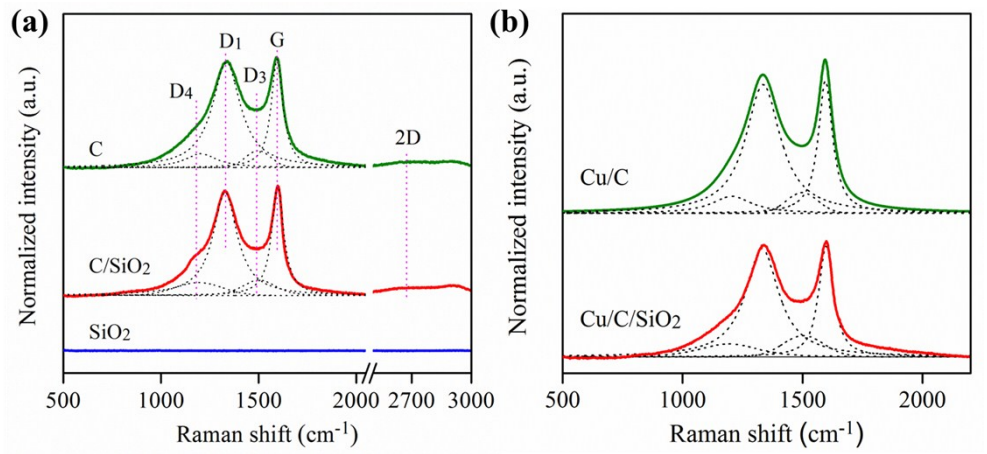

Fig. S7 Raman spectra of the supports and catalysts.

In general, D and G bands are used to indicate the graphitization degree of carbon materials. As reflected by Raman spectroscopy, the intensity ratio of the D to G bands (I_D/I_G) of C/SiO_2 and SiO_2 is 0.96 and 0.94. This amorphous feature of the carbon layer is favorable for the dispersion of Cu species during an impregnation process.[3] Because the intensity ratio of I_D/I_G of $Cu/C/SiO_2$ is nearly equal to that of the C/SiO_2 (0.97 vs. 0.96), the effect of methanation on the nature of the carbon layer is negligible.

8 XPS data

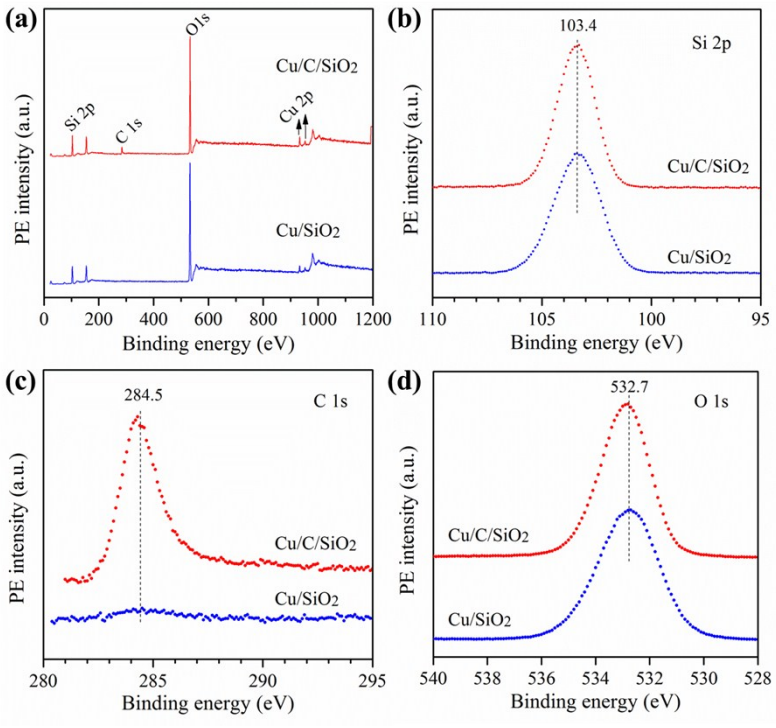

Fig. S8 (a) XPS survey spectra of $Cu/C/SiO_2$ and Cu/SiO_2 catalysts. High-resolution (b) Si 2p, (c) C 1s, and (d) O 1s spectra of these catalysts.

9 CO-DRIFTS spectra

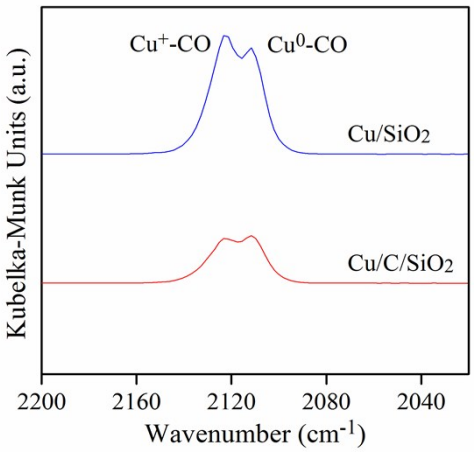

Fig. S9 In situ DRIFTS spectra of CO adsorption at room temperature after purging He 20 min.

10 Stability test

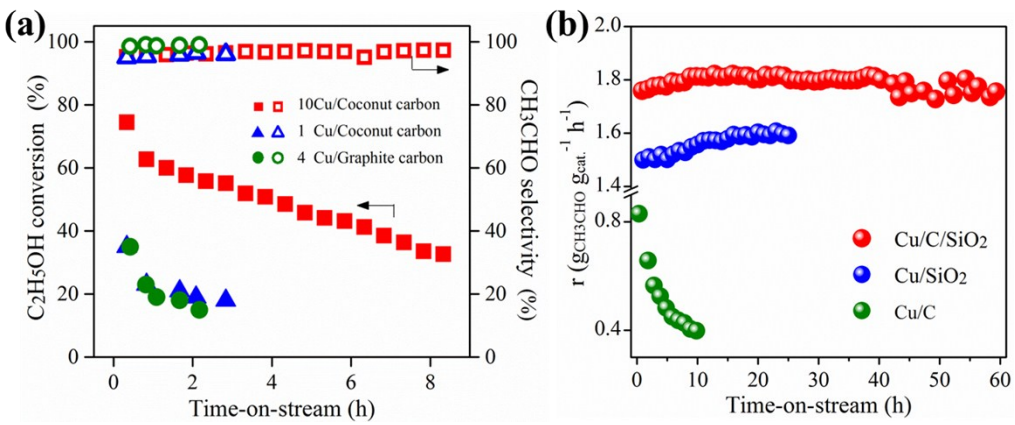

Fig. S10 (a) Stability test of ethanol dehydrogenation over Cu/Carbon catalysts. (b) The acetaldehyde formation rates on Cu/C/SiO_2, Cu/SiO_2, and Cu/C. Reaction conditions: 260 °C, weight hourly space velocity (WHSV) of C_2H_5OH = 2.4 g_{C2H5OH} g_{cat}^{-1} h^{-1}, and N_2 40 mL/min. Reduction: 450 °C for 2 h.

11 Dependence of product selectivity and ethanol conversion on W/F

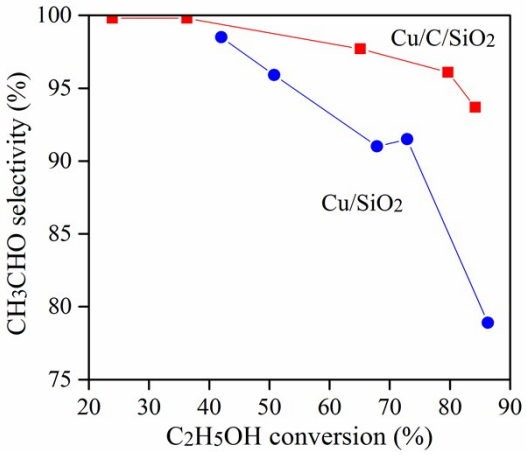

Fig. S11 Dependence of C_2H_5OH conversion and CH_3CHO selectivity in the ethanol dehydrogenation reaction over the reduced catalysts.

12 CH_3CHO-TPD profiles

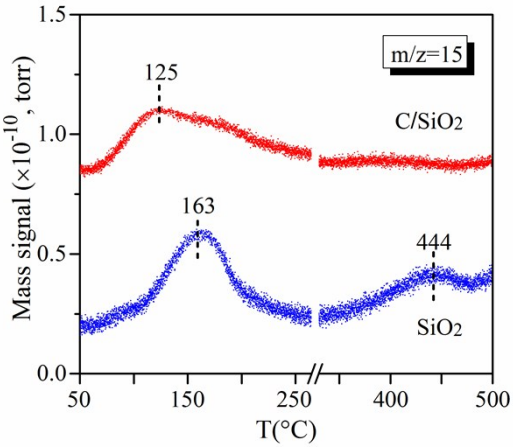

Fig. S12 CH_3CHO-TPD profiles of C/SiO_2 and SiO_2 at m/z = 15.

The main desorption peaks of the C/SiO_2 and SiO_2 supports are at 125 and 163 °C, respectively. This m/z=15 signal attributes to $-CH_3$ groups. Compared with the C/SiO_2 support, there is an apparent desorption peak at ~440 °C on SiO_2. The m/z = 29 ion fragmentation may come from CH_3CHO, C_3H_7CHO, $CH_3COOC_2H_5$, $CH_3COC_2H_5$, etc. By combining these results, one can conclude that by-products are produced from CH_3CHO molecules on the Si-OH groups.

13 Summary of the catalytic data of Cu-based catalysts

Table S1 Summary of the catalytic data of some representative Cu-based catalysts used in the DHEA

No.	Catalysts	T (°C)	WHSV (h^{-1})	Feed composition (%)	Conversion (%)	Selectivity (%)	Yield (%)	TOF (s^{-1})	T[a] (h)	k_D[b] (h^{-1})	τ[c] (h)	Ref.
	8.8 wt% Cu/C/SiO_2	260	2.4	C_2H_5OH = 5, N_2 = 95	83.7-78.5	93.1-98.5	~78	0.019	60	0.001	1000	**This work**
	8.4 wt% Cu/SiO_2	260	2.4	C_2H_5OH = 5, N_2 = 95	86.3-84.3	75.7-82.1	~64.5	0.017	25	0.001	1000	
	8.3 wt% Cu/C	260	2.4	C_2H_5OH = 5, N_2 = 95	36.5-17.5	98.9-99.0	36.0-17.3	0.018[d]	10	0.108	9.2	
1	Cu	320	4.3	C_2H_5OH = 7.6, N_2 = 92.4	90-45	~99	89-44	-	8	0.125	8	[4]
2	10 wt% Cu/Carbon	260	2.4	C_2H_5OH = 5, N_2 = 95	74.8-32.7	~95	71.6	-	8	0.44	6.2	[5]
	10 wt% Cu/N-Carbon	260	2.4	C_2H_5OH = 5, N_2 = 95	80-74.4	~93.7	74.4	-	8	0.0094	106	
3	5 wt% Cu/N-Graphenes	250	3.42	C_2H_5OH = 15, N_2 = 85	67.8-65.3	97	66.8-64.3	-	3	0.013	77	[6]
4	8.5 wt% Cu/5 wt% CoO/2 wt% Cr_2O_3/Asbestos	275	1.9	C_2H_5OH = 100	49.6-42.6	85.1	42-36	-	28	0.006	167	[7]
5	5 wt% Cu/SiO_2	280	-	GHSV = 3600 h^{-1}	53-45	61.0	~32.7	-	10	0.018	56	[8]
	5 wt% Cu/1 wt%K_2O/SiO_2	280	-	GHSV = 3600 h^{-1}	~38	~88	33.4	-	N.D.[e]	-	-	
6	30 wt% Cu/ZnO	160	0.36	C_2H_5OH = 20.5, N_2 = 79.5	~55.0	58.0	32.0	-	N.D.	-	-	[9]

	30 wt% Cu/SiO_2	220	0.36	C_2H_5OH = 20.5, N_2 = 79.5	76.1	21.0	16.0	-	N.D.	-	-	
7	10 wt% Cu/ZrO_2	200	0.83	C_2H_5OH = 28, N_2 = 72	45.0	23.0	10.3	-	N.D.	-	-	[10]
8	30 wt% Cu/SiO_2	220	0.44	C_2H_5OH = 20.5, N_2 = 79.5	~50.0	77.9	39.0	-	N.D.	-	-	[11]
	30 wt% Cu/Al_2O_3	220	0.44	C_2H_5OH = 20.5, N_2 = 79.5	~50.0	54.1	27.1	-	N.D.	-	-	
9	15 wt% Cu/Al_2O_3	300	31.6	C_2H_5OH = 46, N_2 = 54	~80	~86	~68.8	-	N.D.	-	-	[12]
10	10 wt% Cu/SiO_2	280	2.4	C_2H_5OH = 15, N_2 = 85	~83	~68	56.4	-	N.D.	-	-	[13]

[a] t, Reaction time. [b] k_D, second-order deactivation rate constant acquired by fitting the deactivation profile with a second-order deactivation law: $da/dt = -k_D \cdot a^2$, where "a" denotes the normalized yield.[14] [c] Time required for rates to decrease by e^{-1}, $\tau = 1/k_D$. [d] Due to the fast deactivation of Cu/Carbon, the initial conversion value was used by extrapolating the conversion to 0 min. [e] N.D., no detected.

References

1 P. Munnik, M. Wolters, A. Gabrielsson, S. D Pollington, G. Headdock, J. H. Bitter, P. E. de Jongh and K. P. de Jong, *J. Phys. Chem. C* 2011, **115**, 14698–14706.

2 F. W. Chang, H. C. Yang, L. Roselin and W.Y. Kuo, *Appl.Catal. A* 2006, **304**, 30–39.

3 A. Dandekar, R. T. K. Baker and M. A. Vannice, *J. Catal.* 1999, **183**, 131–154.

4 Y.-J. Tu, C. Li and Y.-W. Chen, *J. Chem. Tech. Biotechnol.* 1994, **59**, 141–147.

5 P. Zhang, Q.-N. Wang, X. Yang, D. Wang, W.-C. Li, Y. Zheng, M. Chen and A.-H. Lu, *ChemCatChem* 2016, **9**, 505–510.

6 M. V. Morales, E. Asedegbega-Nieto, B. Bachiller-Baeza and A. Guerrero-Ruiz, *Carbon* 2016, **102**, 426–436.

7 J. Church and H. Joshi, *Ind. Eng. Chem.*, 1951, **43**, 1804–1811.

8 Y. Zhang, Master's thesis, Tianjin University, China, 2007.

9 S.-i. Fujita, N. Iwasa, H. Tani, W. Nomura, M. Arai and N. Takezawa, *React. Kinet. Catal. Lett.* 2001, **73**, 367–372.

10 A. G. Sato, D. P. Volanti, I. C. D. Freitas, E. Longo and J. Bueno, *Catal. Commun.* 2012, **26**, 122–126.

11 N. Iwasa and N. Takezawa, *Bul. Chem. Soc. Jpn.,* 1991, **64**, 2619–2623.

12 W. H. Cassinelli, L. Martins, A. R. Passos, S. H. Pulcinelli, A. Rochet, V. Briois and C. V. Santilli, *ChemCatChem* 2015, **7**, 1668–1677.

13 Q.-N. Wang, L. Shi and A.-H. Lu, *ChemCatChem* 2015, **7**, 2846 –2852.

14 G. Prieto, J. Zěcević, H. Friedrich, K. P. de Jong and P. E. de Jongh, *Nature Mater.* 2013, **12**, 34–39.